nature cell biology

Functional interaction between PML and SATB1 regulates chromatin-loop architecture and transcription of the MHC class I locus

Pavan Kumar P.[1,2,4], Oliver Bischof[2,4], Prabhat Kumar Purbey[1], Dimple Notani[1], Henning Urlaub[3], Anne Dejean[2] and Sanjeev Galande[1,5]

The function of the subnuclear structure the promyelocytic leukaemia (PML) body is unclear largely because of the functional heterogeneity of its constituents. Here, we provide the evidence for a direct link between PML, higher-order chromatin organization and gene regulation. We show that PML physically and functionally interacts with the matrix attachment region (MAR)-binding protein, special AT-rich sequence binding protein 1 (SATB1) to organize the major histocompatibility complex (MHC) class I locus into distinct higher-order chromatin-loop structures. Interferon γ (IFNγ) treatment and silencing of either SATB1 or PML dynamically alter chromatin architecture, thus affecting the expression profile of a subset of MHC class I genes. Our studies identify PML and SATB1 as a regulatory complex that governs transcription by orchestrating dynamic chromatin-loop architecture.

Chromatin architecture has an important role in the regulation of nuclear function[1]. SATB1 organizes chromatin into distinct loops by periodic anchoring of MARs to the nuclear matrix[2]. Furthermore, SATB1 functionally interacts with chromatin modifiers to suppress gene expression through histone deacetylation and nucleosome remodelling at SATB1-bound MARs[3,4]. Although interaction between SATB1 and partner proteins is generally mediated by its amino-terminal PDZ-like domain[4], which is also important for SATB1 homodimerization[5], its MAR-binding- and homeo-domains are indispensable for recognition of MARs[6].

Here, we set out to define more precisely the role of SATB1 in global gene regulation by identifying its partners, and found that it interacted with the PML protein. PML is the single-most important constituent of the PML nuclear body and exists as seven isoforms[7]. PML is a member of a protein family characterized by a RBCC motif consisting of RING finger, B-box and coiled-coil (CC) domains[7]. Posttranslational modification of PML by small ubiquitin-related modifier (SUMO) is required for proper formation of the nuclear bodies and recruitment of nuclear body-associated proteins[8,9]. PML nuclear bodies were shown to associate with the gene-rich region of the MHC-I on chromosome 6p21-22 (ref. 10) and in general, with transcriptionally active loci[11,12]. However, the dynamic nature and subnuclear localization pattern of PML nuclear bodies does not reflect the DNA-binding specificities of any protein among the plethora of proteins associated with them[13].

Using modified *in vivo* chromatin conformation capture (3C) methodology[14,15] combined with chromatin immunoprecipitation (ChIP), we demonstrate that PML and SATB1 act in unison to organize the MHC-I locus into a distinct higher-order chromatin-loop structure by tethering MARs to the nuclear matrix. IFNγ treatment as well as RNA interference (RNAi)-mediated knockdown of *SATB1* and *PML* alter higher-order chromatin structure by modulating the physico-functional association between SATB1, PML and MARs, which alters expression of a subset of MHC-I genes. Our studies support a role for PML–SATB1 complex in governing global gene expression by establishing distinct chromatin-loop architecture.

RESULTS

SATB1 interacts with PML and colocalizes with PML nuclear bodies

To identify interacting partners of human SATB1, a yeast two-hybrid screen was performed using the PDZ-like domain of SATB1 (Fig. 1a) as a bait. Two cDNAs encoding the PML-I protein were isolated (data not shown). Conversely, anti-PML antibody matrix was used to specifically isolate protein complexes containing PML in Jurkat cells. Sequences of two tryptic peptides derived from the proteins in the eluate matched perfectly with that of SATB1 (see Supplementary Information, Fig. S1a), suggesting that SATB1 is one among several proteins that complex with

[1]National Centre for Cell Science, Ganeshkhind, Pune 411007, India. [2]Unité d'Organisation Nucléaire et Oncogénèse/INSERM U579, Institut Pasteur, 28, rue du Docteur Roux, 75724 Paris CEDEX 15, France. [3]Max-Planck-Institute for Biophysical Chemistry, Bioanalytical Mass Spectrometry Group, Am Fassberg 11, D-37077 Goettingen, Germany. [4]These authors contributed equally to this work.
[5]Correspondence should be addressed to S.G. (e-mail: sanjeev@nccs.res.in)

Received 18 August 2006; accepted 8 November 2006; published online 17 December 2006; DOI: 10.1038/ncb1516

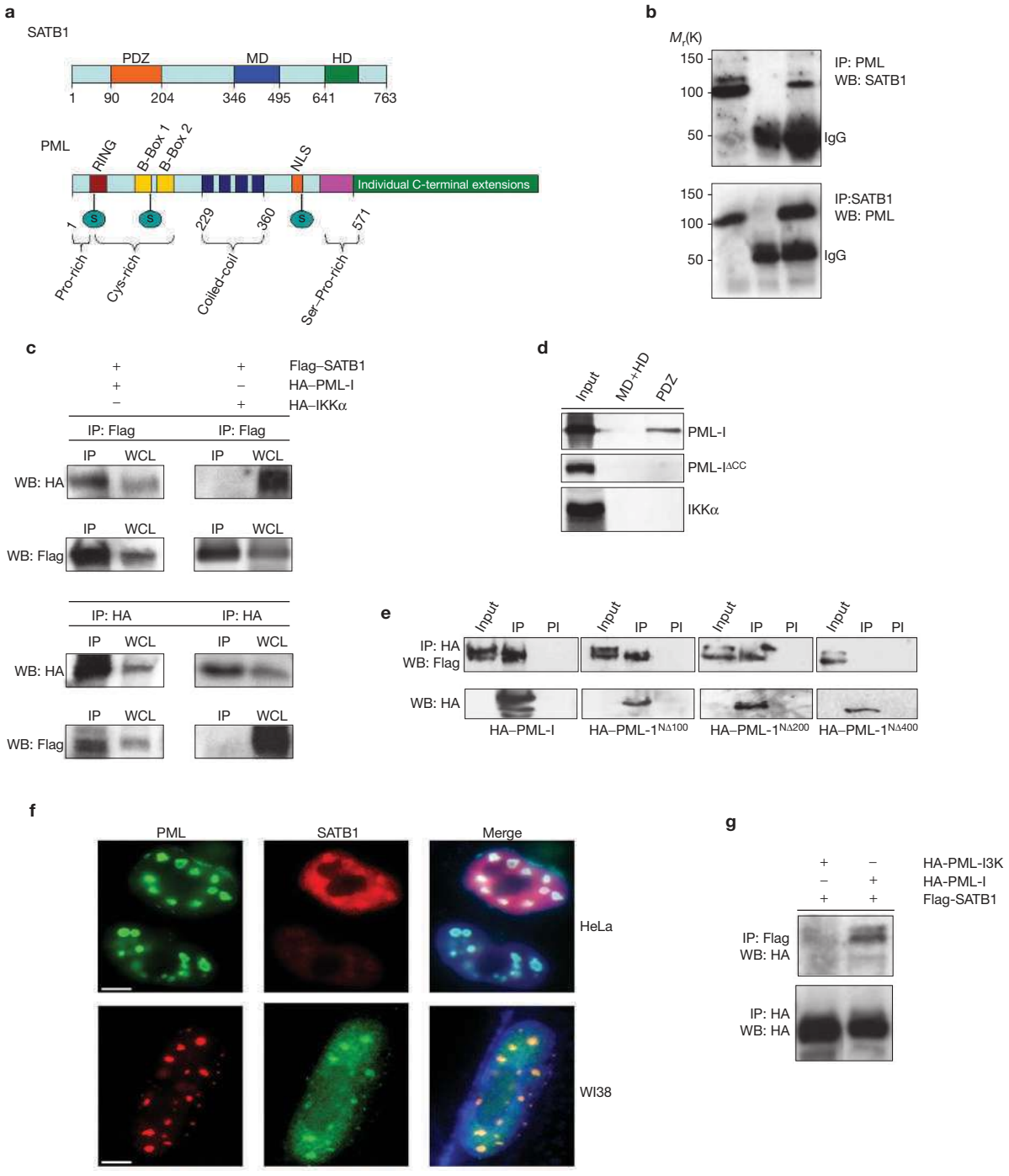

Figure 1 SATB1 and PML interact *in vivo* and *in vitro*. (**a**) Schematic representation of functional domains of SATB1 and PML. Sumoylation sites in PML (S) and alternatively spliced isoforms of PML (variable C-terminal region) are depicted. Amino-acid positions demarcating the domains are indicated. (**b**) Coimmunoprecipitation of endogenous PML and SATB1 in nuclear lysates (10 mg) from Jurkat cells using anti-SATB1, anti-PML, pre-immune (PI) serum or murine IgG control antibodies. Input is 0.5%. (**c**) Coimmunoprecipitation of PML and SATB1 in cell lysates from HEK 293T cells transfected with Flag–SATB1 together with HA–PML-I or HA–IKKα as negative control. Antibodies used for immunoprecipitation (IP) and western blotting (WB) are as indicated. WCL: whole-cell lysate is 50 μg (0.5% of input). (**d**, **e**) The PDZ-domain of SATB1, the coiled-coil domain and sumoylation of PML are indispensable for interaction. GST–MD + HD or GST–PDZ domains of SATB1 immobilized on glutathione beads were incubated with *in vitro* translated, radiolabelled PML-I, PML-I$^{\Delta CC}$ or IKKα as control (d). Bound complexes were analysed by autoradiography. Input, 15%. Coimmunoprecipitation using anti-HA antibody of with HA–PML-I deletion constructs and Flag–SATB1 in cell lysates from transfected HEK 293T cells (**e**). (**f**) Colocalization of PML and SATB1 in PML nuclear bodies. HeLa cells were cotransfected with Flag–SATB1 and HA–PML-I, and costained with anti-HA, anti-Flag antibodies and DAPI. For WI38 primary human-lung fibroblasts, endogenous proteins were detected with anti-PML and anti-SATB1 antibodies. The scale bar represents 1.5 μm. (**g**) Coimmunoprecipitation using anti-Flag antibody of PML and SATB1 in cell lysates from HEK 293T transfected with Flag–SATB1 and HA–PML-I or sumoylation-deficient mutant construct HA–PML-I^{3K}. Uncropped images of all western blots are shown in the Supplementary Information, Fig. S5.

PML. SATB1 and PML-I reciprocally immunoprecipitated each other when antibodies against endogenous proteins (Fig. 1b) or against the tagged proteins (Fig. 1c) were used, suggesting a physical interaction between SATB1 and PML. *In vitro*-binding assays indicated that both the PDZ-like domain of SATB1 and the coiled-coil domain of PML-I (amino acids 229–360, Fig. 1a) are indispensable for this interaction (Fig. 1d). Coimmunoprecipitaion analysis using truncations of HA–PML-I substantiated this observation, by showing that a mutant protein with the amino-terminal 400 amino acids deleted (HA–PML-$I^{N\Delta400}$), which is devoid of the coiled-coil domain, failed to interact with SATB1 (Fig. 1e). Immunofluorescence microscopy analysis revealed that, in HeLa cells ectopically expressing SATB1 and PML-I, SATB1 displayed a diffuse nuclear distribution and accumulated in a number of dot-like structures that coincided with PML-associated nuclear bodies. The colocalization of endogenous SATB1 and PML in PML nuclear bodies was also evident in WI38 fibroblasts (Fig. 1f). We showed that SATB1 is expressed in multiple cell types, including non-T cells (see Supplementary Information, Fig. S1b). In addition, coimmunoprecipitation analysis using extracts from 293T cells transfected with Flag–SATB1 together with HA–PML-I, or the sumoylation-deficient HA–PML-I^{3K} mutant[9] revealed that only wild-type PML, but not the sumoylation-deficient mutant, associated with SATB1 (Fig. 1g). From these data, it is clear that the *in vivo* interaction between the SATB1 and PML occurs in PML nuclear bodies and is dependent on the correct sumoylation of PML.

SATB1 and PML functionally interact at MARs

In electrophoretic mobility shift assay (EMSA) using IgH–MAR probe, only SATB1 formed a complex but PML failed to do so (Fig. 2a), which is in accordance with the known strong affinity of SATB1 for MARs[6] and the lack of DNA-binding activity in PML. In the presence of both proteins, a supershift of the original SATB1–DNA complex was observed (Fig. 2a), suggesting that SATB1, PML and MARs form a trimeric complex, and that PML may enhance the binding of SATB1 to MARs. EMSA using nuclear extract from Jurkat T cells produced a diffused type of complex (Fig. 2b), part of which was supershifted in presence of anti-PML to the well of the gel. A monoclonal antibody raised against a region between the MAR-binding- and homeo-domain led to formation of a distinct supershifted band, whereas an antibody directed against the MAR-binding domain + the homeo-domain inhibited formation of the complex itself, as evidenct from a reduction in the intensity of the complex (Fig. 2b). Interestingly, addition of exogenous PML-I to the nuclear extract retarded the probe in a manner similar to adding anti-PML antibody, suggesting that a macromolecular complex has been formed, thus, further emphasizing the role of PML in formation of larger SATB1–MAR complex(es).

To lend further support to a possible functional interaction between SATB1 and PML, we performed MAR-linked luciferase reporter assays. When individually expressed, SATB1 or PML-I repressed reporter-gene expression approximately threefold (Fig. 2c). Repression by SATB1 was further enhanced by coexpression of PML-I (Fig. 2c). PML-mediated repression was completely obliterated when *SATB1* was specifically silenced by RNAi (Fig. 2c). Furthermore, the repression mediated both by SATB1 and PML-I was observed only with wild-type MAR and not with the mutated MAR that lacks the base-unpairing propensity[16] (Fig. 2d). The enhanced repression observed with coexpression of PML-I and SATB1 was also not observed when mutated MAR-linked reporter was used (Fig. 2d), highlighting the importance of binding to MARs. Taken together, our results strongly suggest a role for PML in modulating MAR function through direct interaction with SATB1.

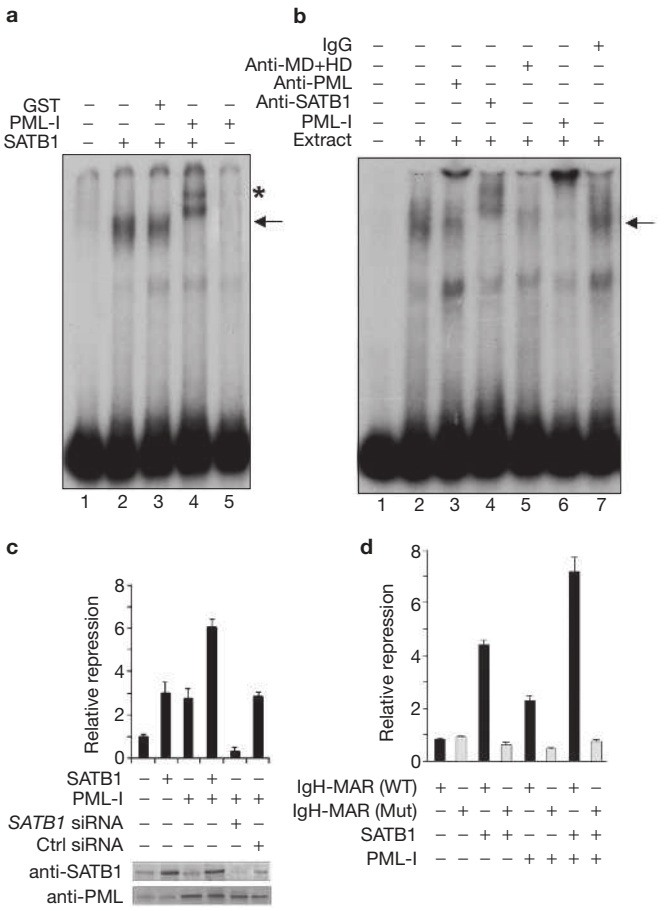

Figure 2 SATB1, PML and MARs form a functional complex. (**a**) EMSA analysis of recombinant SATB1, PML-I and ^{32}P-end-labelled IgH MAR probe *in vitro*. The MAR probe was incubated either with 0.1 μg each of SATB1 (lane 2), 0.1 μg of PML-I (lane 5), or 0.1 μg SATB1 plus 0.1 μg PML-I (lane 4), with addition of GST serving as negative control (lane 3). DNA–protein complexes were resolved on native polyacrylamide gel and visualized by autoradiography. The arrow indicates the band shift corresponding to SATB1–MAR complex and asterisk indicates SATB1–PML–MAR complex. (**b**) Antibody-mediated supershift of SATB1–PML *in vitro*. The MAR probe was incubated with 1.0 μg Jurkat nuclear extract (lane 2), and additionally with anti-PML (lane 3), anti-SATB (lane 4), anti-MD + HD (lane 5), 0.2 μg PML-I (lane 6), or rabbit IgG (lane 6). DNA–protein complexes were resolved on native polyacrylamide gel and visualized by autoradiography. The arrow indicates the band shift corresponding to the SATB1–MAR complex. (**c**) 293T cells were transiently transfected with the indicated expression constructs or siRNA duplexes, together with an IgH MAR–luciferase reporter vector. Ctrl siRNA is a scrambled version of *SATB1* siRNA. Luciferase activity is expressed as fold repression. Data from triplicates are plotted and relative luciferase units are represented as fold activity with respect to the reporter alone. The statistical significance of differences between the treatment groups was calculated using one-way ANOVA and the observed P values were always <0.001. Immunoblot analysis for the expression of SATB1 and PML in the respective transfections is also shown. (**d**) Repression mediated by SATB1 and PML is specific to MARs. 293T cells were transiently transfected with the indicated expression constructs and an IgH MAR–luciferase reporter vector (WT) or its non-MAR mutated version (Mut). Luciferase assay was performed as described in Methods. The error bars represent mean ± s.d. (n = 3).

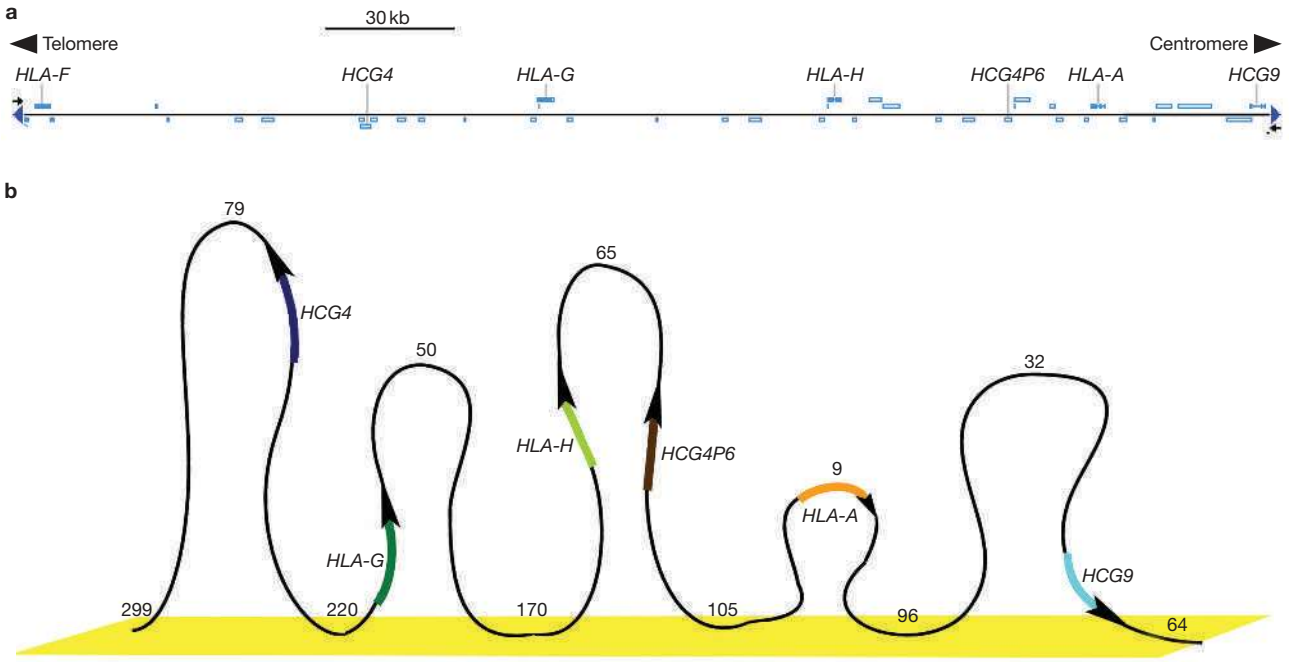

Figure 3 The MHC class I locus is organized into distinct chromatin loops. (**a**) Schematic representation of various genes located in a 0.3 Mb region of the MHC-I locus within the human chromosome 6p21.3 locus flanked by the *HLA-F* and *HCG9* genes, respectively. (**b**) Schematic representation of the *MHC-I* gene locus chromatin-loop organization, as deduced by the MAR-ligation assay (see Methods for details). Relative locations of individual genes studied have been indicated with coloured arrows specifying their transcriptional direction. Numbers on top of the loops indicate size of the loops in kb, whereas numbers at bases of the loops indicate the position of tethered MARs in kb. The yellow coloured platform at the base of the loops indicates the nuclear matrix.

PML and SATB1 are involved in the chromatin-loop organization of the MHC class-I locus *in vivo*

As PML is known to be involved in MHC-I expression[17], we wanted to determine whether PML and SATB1 cooperate in the chromatin-loop organization of a 0.3 Mb region in the MHC-I locus that is flanked by the *HCG9* and *HLA-F* genes (Fig. 3a). Computer-aided analysis[18] predicted two MARs centered at 105 and 299 kb (see Supplementary Information, Fig. S2a). To confirm these MARs *in vivo*, we designed a MAR-ligation assay that, analogous to the 3C methodology[14,15], generates a population-average measurement of juxtaposition frequency between any two genomic loci held together by protein(s), thus, providing information on their relative proximity in the nucleus. The *in vivo* existence of these putative MARs was confirmed by their selective matrix association using specific primers sets. Using these as reference MARs, we then scanned across the entire 0.3 Mb region for additional MARs by applying different primer sets in various combinations (see Supplementary Information, Fig. S2b–f). We conclude that regions surrounding base positions (in kb) 64, 96, 105, 170, 220 and 299 are MARs and that intervening regions loop out (Fig. 3b). To exclude the possibility of selection bias, specific primer sets covering fixed distances across the 300 kb region of the MHC-I locus (see Supplementary Information, Fig. S3a) were also designed and the matrix-loop partitioning assay was performed without any ligation (see Supplementary Information, Fig. S3b). Comparison of the results from this unbiased approach with the results from the software-guided MAR-ligation assay confirmed the positions of MARs as above.

SATB1 and PML are directly associated with the bases of chromatin loops and upstream regulatory sequences of genes within the MHC-I locus

We investigated whether SATB1 and PML could be detected in the vicinity of transcription units within the MHC-I locus *in vivo* by performing locus-wide ChIP analysis using primers against regions at periodic distances within the locus (see Supplementary Information, Fig. S3a). Anti-SATB1 and anti-PML chromatin-immunoprecipitated DNA yielded comparable amplification with 1F–2R, 19F–20R, 17F–18R, 58F–59R, 50F–51R and 3F–4R primer sets, suggesting equal distribution of SATB1 and PML in the corresponding regions of the MHC-I locus (Fig. 4a). Amplifications using other primer sets showed significant differences between anti-SATB1 and anti-PML immunoprecipitated chromatin, indicating that SATB1 is predominantly bound to these regions. Furthermore, primer sets 20F–21R, 37F–38R, 7F–8R and 49F–50R resulted in specific amplifications only with anti-SATB1, but not anti-PML, suggesting that SATB1 independently associates with various regions of the MHC-I locus. We failed to observe any region where PML is associated and SATB1 is not, thus, supporting the hypothesis that SATB1 recruits PML to its genomic targets. Moreover, the two proteins were found to bind, not only canonical MARs, but also to upstream regulatory regions of certain genes within the MHC-I locus in a non-random fashion (Fig. 4d). Taken together, these results imply that SATB1 and PML not only serve as architectural chromatin components, but also as *bona fide* transcriptional regulators for certain MHC-I genes.

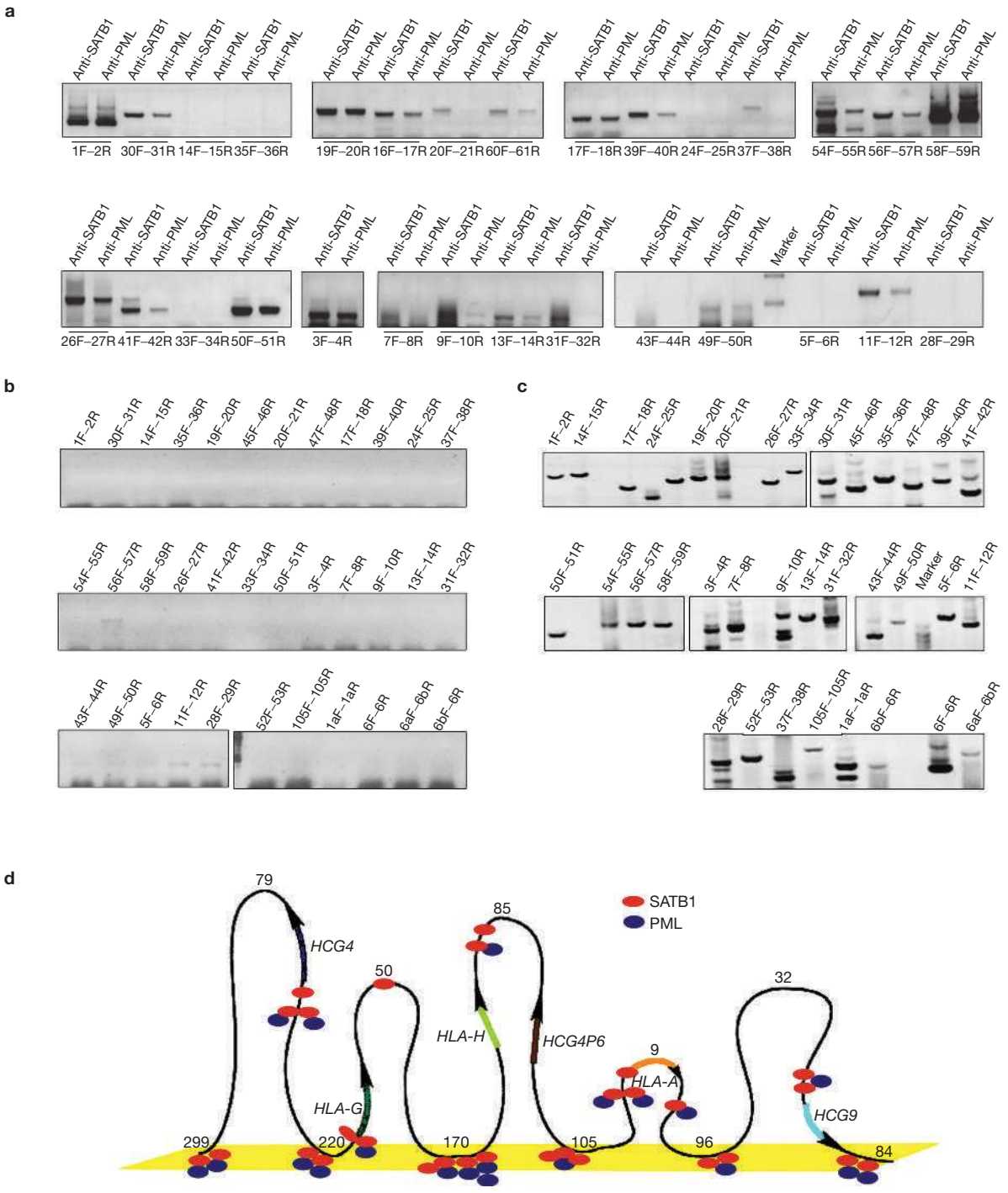

Figure 4 SATB1 and PML directly associate with specific genomic regions of MHC class I locus *in vivo*. (**a**) ChIP assays were performed in Jurkat cells as described in the Methods. The forward (F) or reverse (R) primer sets used are indicated below the panels. Antibodies used for ChIP were anti-SATB1 and anti-PML. The presence of PCR-amplified bands indicates occupancy of protein with the corresponding region of MHC-I locus. (**b**) ChIP assays were performed with rabbit IgG and immunoprecipitated chromatin was amplified with the specific sets of primers indicated above each panel. (**c**) DNA purified from input chromatin was used for PCR amplifications using the primer sets indicated above each panel. (**d**) Schematic representation of occupancy of SATB1 and PML at various locations within the MHC-I locus.

IFNγ treatment induces dynamic reorganization of the chromatin loops

Next, we examined whether PML and SATB1 occupy the newly identified MARs *in vivo* and also whether IFNγ treatment, which is known to induce both PML and MHC-I expression[19,20], alters the higher-order chromatin structure of the MHC-I locus. Specific PCR amplifications with anti-SATB1-precipitated chromatin from untreated Jurkat cells in the ChIP-loop assay[21] suggested SATB1-mediated attachment of all of the previously identified MAR regions (Fig. 5a). In contrast, anti-PML antibody immunoprecipitated MARs only at 105, 170, 220 and 299 kb

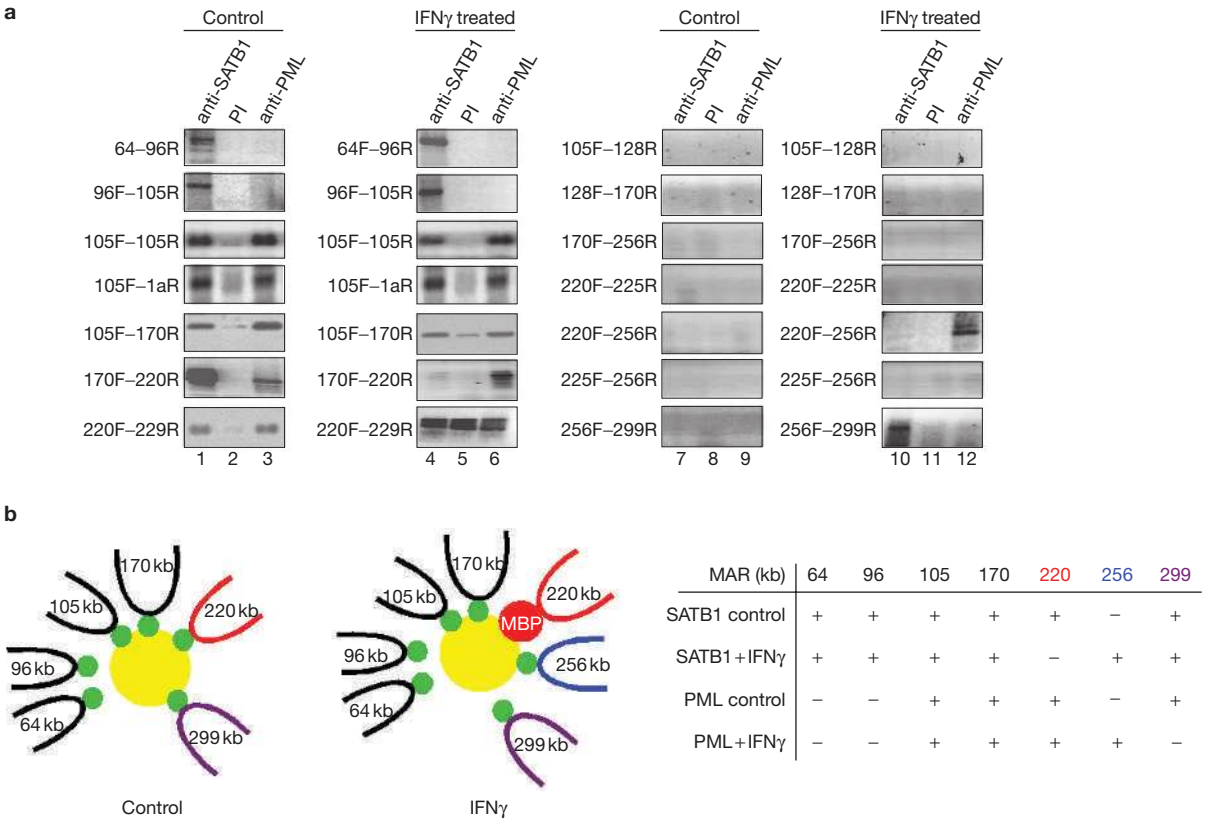

Figure 5 Involvement of SATB1 and PML in the chromatin-loop organization of the MHC class I locus before and after IFNγ treatment. (**a**) PML tethers MHC-I chromatin loops to the nuclear matrix through SATB1 in Jurkat control and IFNγ-treated cells. ChIP-loop assays were performed as described in the Methods. Applied primer sets are indicated on the left of each panel. Primers are in the forward (F) or reverse (R) orientation. Antibodies used for ChIP were rabbit anti-SATB1, anti-PML 83-10 and rabbit pre-immune serum. Presence of PCR-amplified bands indicates matrix attachment of the corresponding regions depicted by the position (in kb) of the primers. In control ChIP reactions (using either primer sets that do not correspond to any MARs within the locus, such as those corresponding to kb positions 128 and 225, or a primer set that does not constitute juxtaposed MARs, such as 170F–256R) no PCR amplifications (lanes 7–12) were observed, confirming that the ChIP-loop assay in general, and the PCR reactions in particular, produce specific results. (**b**) Schematic representation of the predicted chromatin-loop structure of the MHC-I locus in control cells and IFNγ-treated cells, as deduced from the ChIP-loop assay. Base positions of MARs at the bases of each loop are indicated in kb. Loops that are altered in control versus IFNγ-treated cells are indicated by colour coding. Green spheres represent SATB1 and yellow spheres represent PML and its associated nuclear bodies. Unknown MAR-binding protein (MBP) tethering the region around 220 kb is represented as a red sphere. The table summarizes the results of the ChIP-loop assay by listing the presence (+) or absence (–) of MARs at the indicated kb positions.

regions and not at 64 kb and 96 kb regions, as indicated by the reproducible failure of amplifications using primer sets 64F–96R and 96F–105R. On IFNγ treatment, SATB1 was no longer associated with the 220 kb region, but instead associated with a new region at 256 kb, as evident from the absence of amplification products using primer sets 170F–220R and 220F–256R, and appearance of a PCR product using set 256F–299R, suggesting formation of a new loop domain. Associations of SATB1 with other MARs, however, remained unchanged. Anti-PML antibodies immunoprecipitated the 105, 170 and 220 kb regions and the new 256 kb region on IFNγ treatment, but not the 299 kb region. As a consequence of the appearance of the new MAR at 256 kb, the 79 kb-sized loop between MARs at 220 kb and 299 kb is expected to split into two smaller sized loops of 43 and 36 kb each, which are attached to MARs at positions (kb) 220, 256 and 299 (see Supplementary Information, Fig. S4a, b). In conclusion, these data show that SATB1 and PML have decisive, albeit distinct, roles in the chromatin organization of the MHC-I locus, and that IFNγ treatment induces a dynamic reorganization of this structure (Fig. 5b).

Direct interaction between SATB1 and PML is necessary for chromatin-loop organization

To evaluate the importance of direct interaction between SATB1 and PML for chromatin organization of the MHC-I locus, we first performed matrix-loop partitioning assays in control CHO cells and CHO cells complemented with SATB1 — thus matching SATB1 expression of Jurkat cells. Matrix-associated DNA purified from control CHO cells yielded specific PCR amplifications that were mostly absent from DNA in loops (Fig. 6a). On overexpression of SATB1 in CHO cells, PCR amplifications of purified matrix-associated DNA were obtained with most of the primer sets (except 30F–31R, 33F–34R and 50F–51R), suggesting that corresponding regions no longer associated with the nuclear matrix. Additionally, SATB1 overexpression led to the association of regions corresponding to primer sets 13F–14R, 39F–40R and 43F–44R with the matrix. These results indicate that, in CHO cells, complementation with SATB1 results in detachment of regions surrounding 128 and 256 kb from matrix and concomitant formation of a new loop at 220 kb region (Fig. 6c), giving rise to MHC-I loop configuration mirroring that of Jurkat cells (Fig. 3b). In a ChIP-loop assay, anti-SATB1

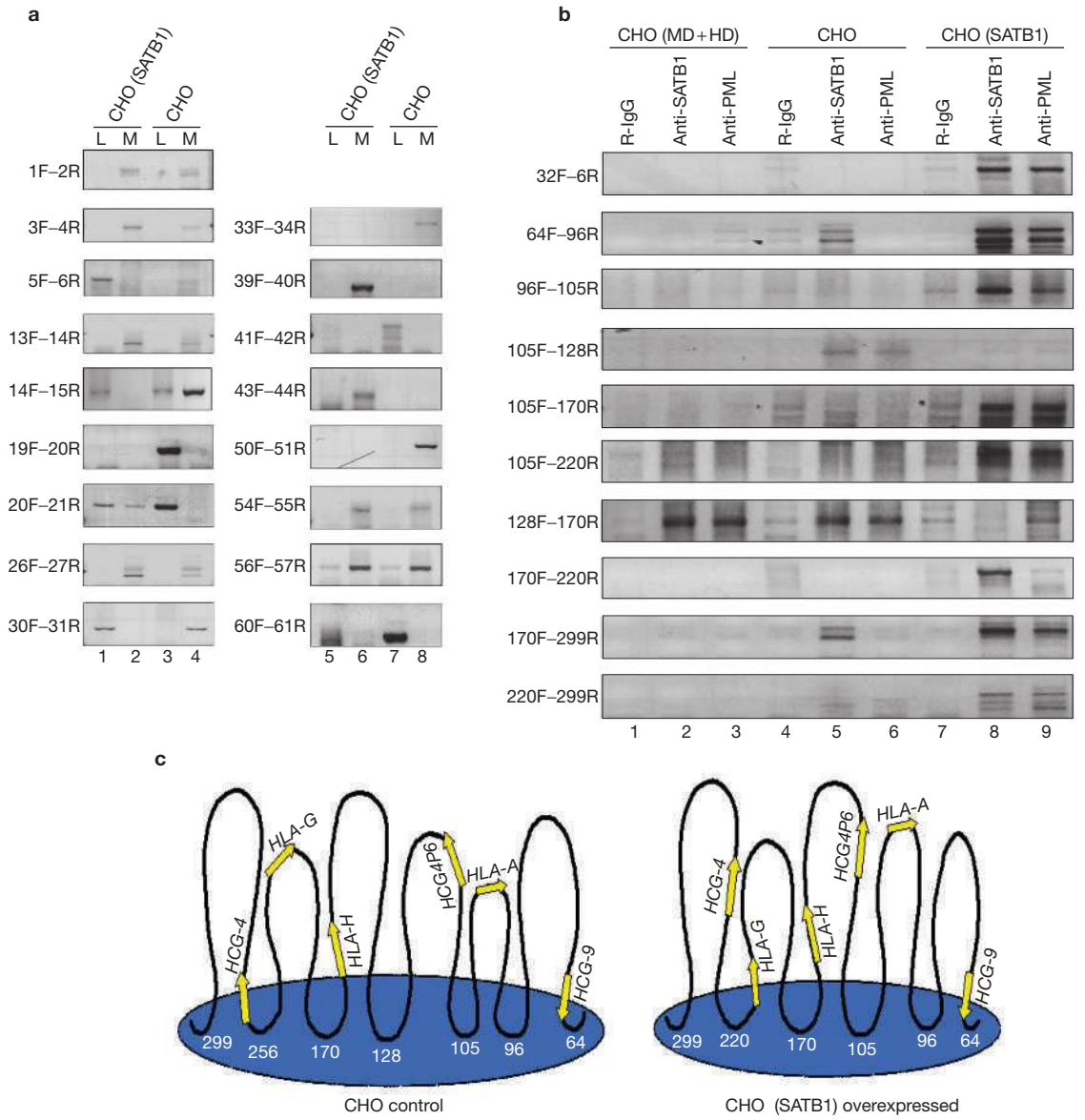

Figure 6 Interaction between SATB1 and PML is required for the distinct chromatin architecture of the MHC class I locus. (**a**) Matrix-loop partitioning assay was performed with CHO control and SATB1-overexpressing CHO cells as described in the Methods. Matrix-bound (lanes 2, 4, 6 and 8) and loop-associated (lanes 1, 3, 5 and 7) DNA was purified and subjected to PCR amplification using unique sets of primers as indicated on the left of each panel. (**b**) SATB1-dependent occupancy of PML at the MHC-I locus in SATB1 overexpressing CHO cells. ChIP-loop assay was performed using control CHO cells (lanes 4, 5 and 6) and CHO cells transfected separately with MD + HD (lanes 1, 2 and 3) and full-length SATB1 expressing constructs (lanes 7, 8 and 9) as described in the Methods. Primer sets used for PCR amplifications are indicated on the left of each panel. Antibodies used for ChIP were anti-SATB1 (lanes , 5 and 8), anti-PML (lanes 3, 6 and 9) and rabbit IgG (lanes 1, 4 and 7). (**c**) Schematic representation of the chromatin-loop structure of the MHC-I locus in control (CHO control) and SATB1-overexpressing CHO cells (CHO SATB1), as deduced from the ChIP-loop assay results.

and anti-PML immunoprecipitated chromatin from control, and MAR-binding- and homeo-domain overexpressing CHO cells failed to show amplification with most of the primer sets (Fig. 6b. The MAR-binding- and home-domain region lacks the PML-interacting PDZ-like domain of SATB1 (Fig. 1a). PCR products derived from anti-SATB1 immunoprecipitated chromatin from control CHO cells indicated attachments to few MARs (Fig. 6b). Despite the existence of abundant PML in CHO cells, anti-PML antibodies failed to display specific association with most of the MAR-elements in the MHC-I locus (Fig. 6b). Furthermore, overexpression of SATB1 in CHO cells restored matrix attachment with most regions, as evident from respective PCR amplifications of anti-SATB1 and anti-PML immunoprecipitated chromatin (Fig. 6b). These data strongly argue that direct interaction between SATB1 and PML is pivotal for establishment of the characteristic chromatin-loop structure at the MHC-I locus.

Collaboration between individual PML isoforms and SATB1 determines the dynamic chromatin organization

Coimmunoprecipitation analysis demonstrated that in addition to PML-I, all other nuclear PML isoforms also interact with SATB1, albeit with different affinities (data not shown). To dissect the roles of individual

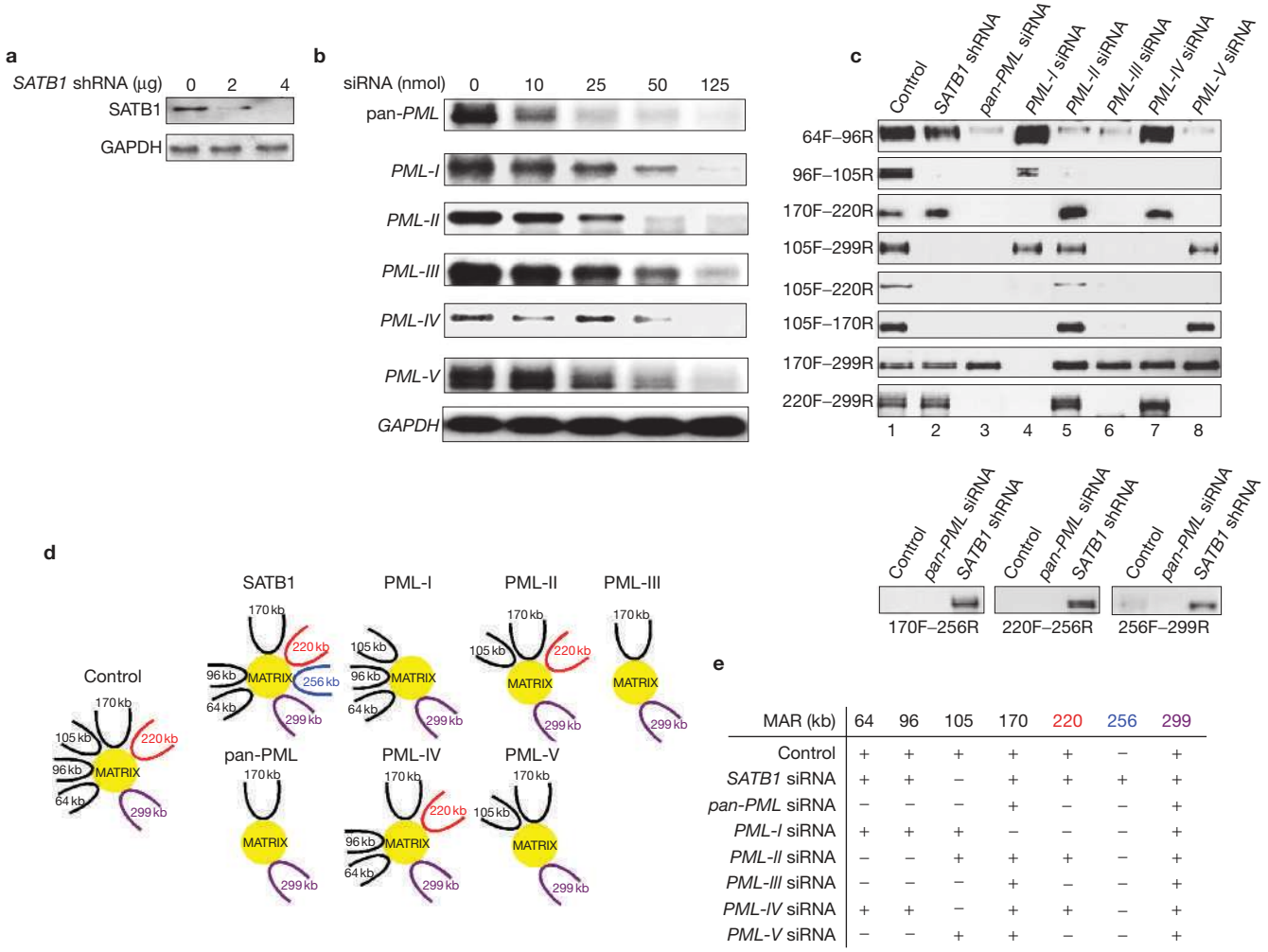

e

MAR (kb)	64	96	105	170	220	256	299
Control	+	+	+	+	+	–	+
SATB1 siRNA	+	+	–	+	+	+	+
pan-PML siRNA	–	–	–	+	–	–	+
PML-I siRNA	+	+	+	–	–	–	+
PML-II siRNA	–	–	+	+	+	–	+
PML-III siRNA	–	–	–	+	–	–	+
PML-IV siRNA	+	+	–	+	+	–	+
PML-V siRNA	–	–	+	+	–	–	+

Figure 7 Compositional balance between SATB1 and individual PML isoforms determines the distinct chromatin architecture of the MHC class I locus. (**a**, **b**) RNAi-mediated silencing of *SATB1* and nuclear *PML* isoforms. RT–PCR analysis of mRNA from Jurkat cells either untransfected or transfected with 2 or 4 μg pSUPER–shSATB1 using primers specific for SATB1 and GAPDH (a). RT–PCR analysis of mRNA from Jurkat cells either untransfected or transfected with 10, 25, 50 or 125 nmol of siRNA duplexes specific for *PML-I–V*, as indicated, or a mixture to silence all isoforms of PML simultaneously (pan-*PML*; **b**). Transcript analysis of *GAPDH* was used as control for gene-specific knockdown using 125 nmol of pan-*PML* siRNA. (c) SATB1 and PML isoforms contribute in specific manners to the chromatin-loop structure of the MHC-I locus. *SATB1* and *PML-I–V* were silenced in Jurkat T cells using RNAi, followed by the MAR-ligation assay as described in the Methods. Matrix-bound DNA was ligated, purified and subjected to PCR amplification using unique sets of primers targeted to discrete regions of the MHC locus in different combinations, as indicated. Jurkat cells (control, lane 1) were transfected separately either with siRNAs or pSUPER–shSATB1 to silence *SATB1* (lane 2), pan-*PML* (lane 3), *PML-I* (lane 4), *-II* (lane 5), *-III* (lane 6), *-IV* (lane 7) and *PML-V* (lane 8). The lower panel indicates results of MAR-ligation assay for the 25 kb IFNγ-inducible loop. (**d**) MARs persisting after silencing of *SATB1*, *PML* or each individual *PML* isoforms are schematically represented by showing the bases of loops attached to the nuclear matrix (in yellow). MAR positions are indicated in kb and loops influenced by IFNγ treatment are colour-coded as in Fig. 5. (**e**) Table summarizing the results of the MAR-ligation assay by listing the presence (+) or absence (–) of matrix attachment for loops at the indicated anchor positions on silencing of *SATB1*, *PML* or each individual *PML* isoforms. IFNγ-affected MARs are colour highlighted as above.

PML isoforms and SATB1 in chromatin-loop organization at the MHC-I locus, matrix-loop partitioning assays were performed using Jurkat cells where *PML* isoforms and *SATB1* were individually silenced (Fig. 7a, b). Matrix-associated DNA yielded specific amplifications with primer sets corresponding to the MARs (Fig. 7c). Matrix-loop partitioning on silencing of *SATB1* demonstrated the strict requirement for SATB1 in the attachment of the 105 kb region (Fig. 7c). In a manner identical to IFNγ treatment (Fig. 5), *SATB1* knockdown resulted in formation of a new loop by anchorage of the region around 256 kb (Fig. 7). Simultaneous knockdown of all *PML* isoforms (pan-*PML*) induced a dramatic change in the loop organization when compared with the *SATB1* knockdown, and only a single primer set, 170F–299R, yielded specific amplification (Fig. 7c). Failure to obtain PCR amplification with the rest of the primer sets on *PML* loss suggests that anchoring of regions around positions 64, 96, 105 and 220 kb to the nuclear matrix is dependent on PML

Using MAR-ligation assays, we then assessed the contribution of individual PML isoforms to the organization of MHC-I higher-order chromatin structure. PCR amplifications using ligated matrix-associated chromatin from cells in which individual *PML* isoforms were silenced indicated their differential contribution in loop-domain organization of MHC locus (Fig. 7c). Among all nuclear PML isoforms, PML-III seems to be the master organizer, as PCR amplifications in *PML-III* knockdown cells mimicked those in pan-*PML* knockdown. The predicted loop structures formed on silencing of *SATB1*, *PML* or each individual

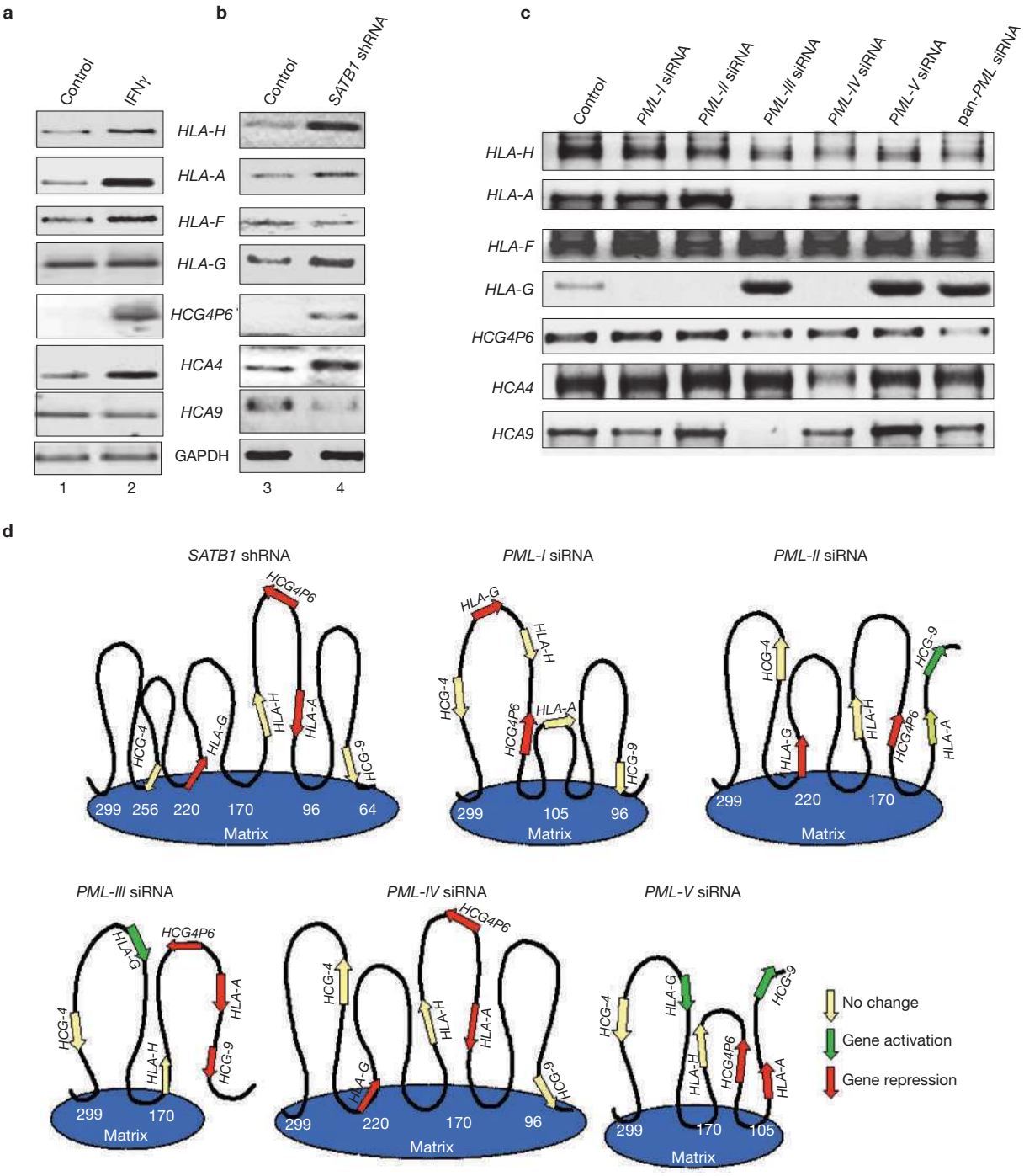

Figure 8 SATB1–PML-mediated chromatin-loop architecture regulates transcription of specific *MHC- I* genes. (**a**, **b**) Silencing of SATB1 mimics the effect of IFNγ treatment. RT–PCR analysis of Jurkat control (lane 1) and IFNγ-treated cells (lane 2) using primers specific for *HLA-H, HLA-A, HLA-F, HLA-G, HCG4P6, HCG4, HCG9* and *GAPDH* (**a**). RT–PCR analysis of Jurkat control (lane 3) and pSUPER–shSATB1 transfected cells (lane 4) using primers as in **a** (**b**). (**c**) Differential effects of *PML* isoform-specific *in vivo* knockdown on the expression of *MHC-I* genes. RT–PCR analysis of mRNA from Jurkat control cells and cells transfected either with 125 nmol *PML-I, -II, -III, -IV, -V* or pan-*PML* siRNAs using gene-specific primers against *MHC-I* genes as in **a**. (**d**) Differential contribution of PML isoforms I–V and SATB1 to chromatin-loop architecture of the MHC-I locus and the impact on transcription. Alterations in chromatin-loop structure were monitored on specific knockdown of *PML* nuclear isoforms *I–V* (see Fig. 6). The loop structures formed according to the specific nuclear matrix attachments are schematically represented and the activity status of genes is indicated. Arrows represent individual genes and indicate the direction of transcription. The nuclear matrix is depicted in blue and the numbers at the bases of loops indicate MAR positions in kb.

PML isoform are schematically depicted in Fig. 7d and summarized in tabular form in Fig. 7e. Taken together, our results clearly demonstrate that a unique interplay exists between PML and SATB1, as well as a striking specificity in the contribution of various PML isoforms — both of which are responsible for determining the unique structural chromatin signature of the MHC-I locus.

IFNγ treatment and silencing of *SATB1* or *PML* isoforms alter the expression profile of a distinct set of MHC-I genes

Chromatin reorganization and transcriptional activity are coupled events[1] and therefore we examined the transcriptional profile of this locus before and after IFNγ treatment, as well as after *SATB1* and *PML* knockdown. IFNγ treatment resulted in upregulation of most of the MHC-I genes, except HCG-9 (Fig. 8a). Moreover, silencing of *SATB1* also selectively altered the transcriptional activity of the MHC genes in a manner that mirrored alterations in gene expression obtained after IFNγ treatment (Fig. 8b). We then studied the influence of each PML isoform on the transcriptional regulation of individual MHC-I genes by performing RT–PCR analysis from cells where expression of all or individual *PML* isoforms were silenced. Expression of *HLA-H*, *HLA-F* and *HCG-4P6* was only slightly affected after inactivating *PML* isoforms *I-V*, either individually (Fig. 8c) or altogether (Fig. 8c). In contrast, expression of *HCG-9*, *HLA-A*, *HCG*-4 and *HLA-G* revealed profound differences on selective silencing of individual *PML* isoforms (Fig. 8c). Expression of *HLA-A* was abrogated when *PML-III* or *PML-V* were knocked down and *HCG*-4 expression was diminished when *PML-IV* was silenced. The most dramatic changes were evident in the expression profiles of *HLA-G* in an isoform-dependent manner. *HLA-G* expression was upregulated with respect to control when *PML-III* and *PML-V* were silenced, whereas the same gene was completely repressed when *PML* isoforms *-I*, *-II*, and *-IV* were inactivated. Thus, these results suggest that individual PML isoforms contribute in diverse manners to the loop-domain organization and regulation of MHC-I expression (Fig. 8d). □

DISCUSSION

We demonstrate that direct interaction between SATB1 and PML is necessary and sufficient for the characteristic loop structure of the MHC locus. We have coined a new term, 'loopscape', to describe the dynamic loop organization at any chromosomal locus. Our findings provide strong support for the idea that PML–SATB1 complexes act as seeding points for the initiation of global transcriptional domains by defining the chromatin loopscape. In contrast with the prevalent notion that PML nuclear bodies form at sites with high transcription activity[12,22], our data argues in favour of a model that implicates their active recruitment to specific genomic loci in a manner reminiscent to that of the nucleolus[23]. PML isoforms have been shown to associate differentially with certain proteins[24,25], hence, altering the PML isoform content of PML nuclear bodies may not only affect the factors that will be recruited to these bodies, but also modulate their nuclear positioning and functional interaction with chromatin. The composition of PML nuclear bodies is highly heterogeneous and PML itself is a dynamic component of PML nuclear bodies[22,26,27] and the nuclear matrix[28]. Thus, PML isoform composition is likely to have a key role in PML nuclear body positioning and overall function in chromatin organization and related nuclear processes.

Chromatin looping may be involved in long-distance gene regulation by locus control regions (LCRs)[29] or MARs[21]. Recently, chromatin looping and its impact on gene regulation were described for the β-globin locus[30], cytokine gene cluster[31], IGF2 (ref. 32) and Dlx5 loci[21]. To monitor the effect of such long-distance interactions on expression of the MHC-I locus, we treated cells with IFNγ, which is a potent inducer of both MHC and PML expression[19,20]. It has been speculated that the megabase-sized giant loops formed after IFNγ induction of MHC-I expression contain multiple smaller loops that are likely to be attached or adjacent to transcription factories[33]. We are now able to incorporate a causal relationship between chromatin-loop reorganization after IFNγ treatment and gene regulatory events mediated by SATB1 and PML. SATB1 seems to be specifically involved in the activation of *HCG-9*, whereas it represses most other genes within the MHC-I locus. Interestingly, the activation status of *HCG-9* is further enhanced if it is pushed into being part of the giant loop formed by dynamic reorganization in that region. Similarly, the positioning of *HCG-4* with respect to the nuclear matrix influences its expression. Locus-wide ChIP analysis suggested that the occupancy of SATB1 and PML is non-random across the MHC-I locus, but instead is clustered at MARs and the upstream regulatory elements. SATB1 has been shown to bind directly to promoters and regulate transcription by recruiting various coactivators and corepressor[4,34,35]. In addition, SATB1 itself is subject to posttranslational modifications that result in different binding affinities for transcriptional regulators and DNA[35]. The effect of posttranslational modification(s) of SATB1 and PML on their physical association with each other could provide an additional layer of regulation and requires further investigation.

The involvement of PML nuclear bodies in regulation of genes with which they are spatially associated is a matter of debate. Pan-*PML* knockdown did not preferentially alter transcription levels of genes that were closer to PML nuclear bodies, or other IFN-responsive of genes such as *HLA-A*, *-B* and *-C*[17,36,37]. PML loss does not seem to affect the majority of classical MHC-I genes involved in antigen presentation[17,36,37], but affects other subsets of MHC-I genes whose functions have not been resolved to date[38]. Although pan-*PML* and *PML-III* knockdown have an identical outcome with regard to chromatin-loop organization, yet the impact on transcriptional regulation of MHC-I genes is very different. The role of the dynamic association of specific MARs within this locus to the matrix is not known. If *HLA-G* is positioned in the vicinity of the matrix, it is downregulated. However, if it is positioned away from the base of the loop, then its transcription is augmented. On the contrary, *HCG-4P6* exists in a constitutively repressed state and therefore affects the expression status of neighbouring genes, such as *HLA-4*. Notably, SATB1 and PML do not bind within 5 kb upstream or downstream of *HCG-4P6*, however they do occupy positions immediately upstream of *HLA-A* and *HLA-G*. Thus, the occupancy of *cis* elements and organization of higher-order chromatin structure by SATB1 and PML are both crucial for regulation of gene expression.

In conclusion, we propose that the SATB1 network and PML nuclear bodies intersect at the MHC-I locus to regulate the coordinated expression of a subset of *MHC-I* genes. This assembly of data is unprecedented in that it actively links PML and PML nuclear bodies to higher-order chromatin organization and transcription. In a manner similar to the active chromatin hub[39], interactions between *cis* elements, such as the promoter and the MAR, in the vicinity may dictate the transcriptional status of the gene(s). The effect of micro-heterogeneity of PML nuclear bodies on the dynamic chromatin organization of multiple gene loci under different physiological conditions offers the next challenge to understand *in toto* the function(s) of PML and PML nuclear bodies.

METHODS

Vectors and cells. The primary human lung fibroblast strain, WI38, was cultured as previously described[24]. The lymphoblastoid T-cell line Jurkat and haematopoietic leukemia cell line NB-4 were cultured in RPMI medium with 10% FBS in 10% CO_2 at 37 °C. pSG5–HA–PML-I, pSG5–PML-I$^{\Delta CC}$ and pSG5–PML-I^{3K} constructs were derived by standard procedures. pCMV10–3×Flag–SATB1 has been described previously[4].

EMSA. EMSAs were performed as previously described[40]. Binding reactions were performed in a 10 µl total volume containing 10 mM HEPES at pH 7.9, 1 mM DTT, 50 mM KCl, 2.5 mM $MgCl_2$, 10% glycerol, 0.5 µg of double-stranded poly (dI-dC), 10 µg BSA and 0.1 µg of the recombinant protein(s). Samples were pre-incubated at room temperature for 5 min before the addition of ^{32}P-labelled IgH–MAR probe. After 15 min incubation at room temperature, the products of such binding reactions were then resolved by 6% native polyacrylamide gel electrophoresis. For protein- or antibody-mediated supershifts, reaction mixtures were incubated for 5 min after the addition of probe and then the protein or antibody was added, incubated further for 10 min at room temperature followed by electrophoresis. The gels were dried under vacuum and exposed to X-ray film.

Protein expression and *in vitro* binding assays. GST–MD+HD (MAR-binding domain + homeo-domain) or GST–PDZ domains of SATB1 and 6×His-tagged full-length SATB1 were expressed in BL21DE *Escherichia coli* and purified according to standard procedures. GST pulldown assays were performed on *in vitro*-translated, ^{35}S-methionine-labelled PML-I and IKKα as previously described[25]. Bound complexes were washed under stringent conditions, eluted, resolved by SDS–PAGE and analysed by autoradiography.

Matrix-loop partitioning assay. This assay identifies the *in vivo* location of any genomic locus, either as nuclear matrix- or loop-DNA-associated. Nuclear matrix- and loop-associated pools of genomic DNA were prepared as previously described[41], with minor modifications. Briefly, Jurkat cells were washed with phosphate buffer followed by sequential lysis with CSK-1 (0.5% triton X-100, 10 mM PIPES at pH 6.8, 100 mM NaCl, 300 mM sucrose, 3 mM $MgCl_2$, 1 mM EGTA, 1 mM PMSF and 1× protease inhibitor cocktail) and CSK-2 buffers (same as CSK-1 except that triton X-100 is omitted). Restriction enzymes (*EcoR*I, *BamH*I, *Hind*III, *Sau3A*I and *Pst*I) were added and digestion was performed for 14 h to digest genomic DNA into approximately 300–500 bp fragments. Digested supernatant (loop DNA), as well as pellet containing undigested material (nuclear matrix + MARs), were independently collected, the restriction enzymes were inactivated by heating at 80 °C for 1 h, and DNA was purified by proteinase K digestion followed by phenol–chloroform extraction and ethanol precipitation. Isolated pools of matrix- or loop-associated DNAs were used as templates for PCR amplification with different sets of primers designed for the MHC-I locus. PCR products were resolved by native polyacrylamide gel electrophoresis, stained with Sybr Gold (Molecular Probes, Eugene, OR) and visualized by UV transillumination.

MAR-ligation assay. The principle of this assay is essentially derived from the 3C methodology[14,15]. However, the obligatory crosslinking step of the 3C assay, which introduces a lot of background noise, is omitted. Nuclear matrix- and loop-associated pools of chromatin were prepared as described above until the restriction digestion step. After heat inactivation of restriction enzymes, the reaction mixtures were diluted threefold and were ligated using T4 DNA ligase for 14 h at 16 °C. DNA was then recovered from the ligation mixtures by proteinase K digestion followed by phenol–chloroform extraction and ethanol precipitation and was used as a template for PCR amplification with different sets of primers (see Supplementary Information, Methods) designed to correspond to regions spanning fixed distances across the MHC-I locus, or for regions surrounding the computer-predicted MARs. PCR products were resolved by native polyacrylamide gel electrophoresis, stained with Sybr Gold and visualized by UV transillumination. All ligation products were confirmed by sequencing the respective PCR amplification products.

ChIP-loop assay. Jurkat cells were crosslinked for 10 min at 25 °C by adding formaldehyde (to a final concentration of 1%) directly to the culture medium and the ChIP-loop assay was performed as previously described[21]. Briefly, after cell lysis, chromatin was sonicated such that genomic DNA was sheared into 500–2000 bp fragments. Sheared chromatin was immunoprecipitated with anti-SATB1 (ref. 42) and anti-PML 83–10 antibodies[43], followed by overnight ligation, reverse crosslinking with 4 M NaCl for 4 h at 65 °C and proteinase K digestion. One tenth of the DNA from each pool was PCR amplified in 50 µl reactions containing 50 mM KCl, 10 mM Tris–HCl, 1.5 mM $MgCl_2$, 0.1% Triton X-100, 1.0 U Taq DNA polymerase (Promega, Madison, WI) and 1 µM of different MHC-I specific primer pairs using one cycle of 95 °C for 5 min, 30 cycles of 95 °C for 1 min, 55–65 °C (depending on the primer pair in use) for 1 min and 72 °C for 1 min. PCR products were resolved by native polyacrylamide gel electrophoresis, stained with Sybr Gold and visualized under UV illumination.

Coimmunoprecipitation, immunoblotting and antibodies. Whole-cell extracts were prepared using extraction buffer (20 mM Tris–HCl at pH 7.6, 200 mM NaCl, 1 mM EDTA, 0.5% NP-40 and 1 mM DTT) supplemented with protease inhibitor cocktail (Roche, Mannheim, Germany). Nuclear extracts were prepared essentially as previously described[4]. For immunoprecipitations, equal amounts of lysate (containing 5–10 mg of total cellular protein or 30 mg of nuclear lysates in the case of Jurkat cells) were pre cleared with rabbit IgG (Sigma, St Louis, MO) and protein A/G plus beads (Pierce, Rockford, IL). Precleared extracts were incubated either with 2 µg rabbit anti-SATB1 (ref. 42), rabbit anti-PML 83–10 (ref. 43), mouse monoclonal (mAb) anti-PML 5E10 (ref. 44), mouse mAb anti-PML PG-M3 (Santa Cruz Biotechnology, Santa Cruz, CA), mouse mAb anti-Flag M2 antibody (Sigma) or mouse mAb anti-HA (Convenance, Richmond, CA) plus Protein A/G beads (Pierce) for 3 h at 4 °C. Precipitates were washed extensively in extraction buffer, bound complexes eluted with 2× SDS–PAGE sample buffer and resolved by 4–15% SDS–PAGE. Immunoblotting was performed according to standard procedures and proteins detected with the indicated antibodies. When immunoprecipitation was not performed, total protein lysates were prepared in 2× SDS–PAGE sample buffer and 50 µg protein were separated by 4–15% SDS–PAGE. Antibodies were detected by chemiluminescence using Galactostar (Tropix, Bedford, MA).

Luciferase-reporter assays. Luciferase assays were performed using Luc Lite reagent (Perkin Elmer, Boston, MA) as previously described[4] and luciferase activity was measured using Top Count (Packard, Downer's Grove, IL). The IgH–MAR–luciferase reporter construct[45] was cotransfected with 3×Flag–SATB1(pSG5–HA–PML-I at 1–2 µg per well, either singly or in different combinations, together with the reporter construct at 1 µg per well. HEK 293 cells were seeded at 0.2×10^6 cells per well and transfected using Lipofectamine 2000 reagent (Invitrogen, Carlsbad, CA). Fold differences were calculated by normalizing the treatment values to the control value. The statistical significance of differences between the groups was calculated using one-way ANOVA (SigmaStat, SPSS Inc., Chicago, IL).

RNAi of *SATB1* and *PML*. Jurkat T-cell suspension cultures were transfected either with siRNAs for selectively knocking down the expression of *SATB1* (Santa Cruz Biotechnology), pan-*PML* and individual *PML* isoforms (Proligos, Lyon, France) or with pSUPER–short hairpin (sh)-*SATB1* using siIMPORTER transfection reagent (Upstate Technologies, Temecula, CA; see Supplementary Information, Methods). The highest siRNA concentration used (125 nmoles) provided the maximum knockdown of each *PML* isoform without affecting cell viability and thus was chosen for analysis. Jurkat cells were seeded in 6-well plates at density of 1×10^6 cells per well. siIMPORTER transfection reagent was used at a concentration of 5 µl per well. Cells were then cultured at 37 °C in a 5% CO_2 atmosphere for 48 h. Subsequently, cells were harvested, RNA was extracted using TRI reagent (Sigma) and was used for RT–PCR analysis.

Note: Supplementary Information is available on the Nature Cell Biology website.

ACKNOWLEDGMENTS

We thank C. Maki for PML amino-terminal deletion constructs, F. Mercurio for pcDNA–IKKα and T. Kohwi-Shigematsu for anti-SATB1. Work was supported by grants from the Department of Biotechnology, Government of India, the Wellcome Trust, UK, the Ligue Nationale Contre le Cancer, the Fondation de France, the European Economic Community 'Intact', and the Association Laurette Fugain. O.B. is a senior research fellow from the Centre National de la Recherche Scientifique. P.K., D.N. and P.K.P are supported by fellowships from the Council of Scientific and Industrial Research, India. S.G. is an international senior research fellow of the Wellcome Trust.

COMPETING FINANCIAL INTERESTS

The authors declare that they have no competing financial interests.

Published online at http://www.nature.com/naturecellbiology/
Reprints and permissions information is available online at http://npg.nature.com/reprintsandpermissions/

1. Spector, D. L. The dynamics of chromosome organization and gene regulation. *Annu. Rev. Biochem.* **72,** 573–608 (2003).
2. Cai, S., Han, H. J. & Kohwi-Shigematsu, T. Tissue-specific nuclear architecture and gene expression regulated by SATB1. *Nature Genet.* **34,** 42–51 (2003).
3. Yasui, D., Miyano, M., Cai, S., Varga-Weisz, P. & Kohwi-Shigematsu, T. SATB1 targets chromatin remodelling to regulate genes over long distances. *Nature* **419,** 641–645 (2002).

4. Kumar, P. P., Purbey, P. K., Ravi, D. S., Mitra, D. & Galande. S. Displacement of SATB1-bound histone deacetylase 1 corepressor by the human immunodeficiency virus type 1 transactivator induces expression of interleukin-2 and its receptor in T cells. *Mol. Cell Biol.* **25,** 1620–1633 (2005).
5. Galande, S., Dickinson, L. A., Mian, I. S., Sikorska, M. & Kohwi-Shigematsu, T. SATB1 cleavage by caspase 6 disrupts PDZ domain-mediated dimerization, causing detachment from chromatin early in T-cell apoptosis. *Mol. Cell Biol.* **21,** 5591–5604 (2001).
6. Dickinson, L. A., Dickinson, C. D. & Kohwi-Shigematsu, T. An atypical homeodomain in SATB1 promotes specific recognition of the key structural element in a matrix attachment region. *J. Biol. Chem.* **272,** 11463–11470 (1997).
7. Jensen, K., Shiels, C. & Freemont, P. S. PML protein isoforms and the RBCC/TRIM motif. *Oncogene* **20,** 7223–7233 (2001).
8. Seeler, J. S. & Dejean, A. Nuclear and unclear functions of SUMO. *Nature Rev. Mol. Cell Biol.* **4,** 690–699 (2003).
9. Zhong, S. *et al.* Role of SUMO-1-modified PML in nuclear body formation. *Blood* **95,** 2748–2752 (2000).
10. Shiels, C. *et al.* PML bodies associate specifically with the MHC gene cluster in interphase nuclei. *J. Cell Sci.* **114,** 3705–3716 (2001).
11. Zhong, S., Salomoni, P. & Pandolfi, P. P. The transcriptional role of PML and the nuclear body. *Nature Cell Biol.* **2,** E85–E90 (2000).
12. Wang, J. *et al.* Promyelocytic leukemia nuclear bodies associate with transcriptionally active genomic regions. *J. Cell Biol.* **164,** 515–526 (2004).
13. Negorev, D. & Maul, G. G. Cellular proteins localized at and interacting within ND10/PML nuclear bodies/PODs suggest functions of a nuclear depot. *Oncogene* **20,** 7234–7242 (2001).
14. Dekker, J., Rippe, K., Dekker, M. & Kleckner N. Capturing chromosome conformation. *Science* **295,** 1306–1311 (2002).
15. Splinter, E., Grosveld, F. & de Laat, W. 3C technology: analyzing the spatial organization of genomic loci *in vivo*. *Methods Enzymol.* **375,** 493–507 (2004).
16. Kohwi-Shigematsu, T., Maass, K. & Bode, J. A thymocyte factor SATB1 suppresses transcription of stably integrated matrix-attachment region-linked reporter genes. *Biochemistry* **6,** 12005–12010 (1997).
17. Zheng, P. *et al.* Proto-oncogene PML controls genes devoted to MHC class I antigen presentation. *Nature* **396,** 373–376 (1998).
18. Singh, G. B., Kramer, J. A. & Krawetz, S. A. Mathematical model to predict regions of chromatin attachment to the nuclear matrix. *Nucleic Acids Res.* **25,** 1419–1425 (1997).
19. Lavau, C. *et al.* The acute promyelocytic leukaemia-associated *PML* gene is induced by interferon. *Oncogene* **11,** 871–876 (1995).
20. Boehm, U., Klamp, T., Groot, M. & Howard, J. C. Cellular responses to interferon-γ. *Annu. Rev. Immunol.* **15,** 749–795 (1997).
21. Horike, S., Cai, S., Miyano, M., Cheng, J. F. & Kohwi-Shigematsu, T. Loss of silent-chromatin looping and impaired imprinting of DLX5 in Rett syndrome. *Nature Genet.* **37,** 31–40 (2005).
22. Kiesslich, A., von Mikecz, A. & Hemmerich, P. Cell cycle-dependent association of PML bodies with sites of active transcription in nuclei of mammalian cells. *J. Struct. Biol.* **140,** 167–179 (2002).
23. Platani, M. & Lamond, A. I. Nuclear organisation and subnuclear bodies. *Prog. Mol. Subcell. Biol.* **35,** 1–22 (2004).
24. Bischof, O., Nacerddine, K. & Dejean, A. Human papillomavirus oncoprotein E7 targets the promyelocytic leukemia protein and circumvents cellular senescence *via* the Rb and p53 tumor suppressor pathways. *Mol. Cell Biol.* **25,** 1013–1024 (2005).
25. Fogal, V. *et al.* Regulation of p53 activity in nuclear bodies by a specific PML isoform. *EMBO J.* **19,** 6185–6195 (2000).
26. Wiesmeijer, K., Molenaar, C., Bekeer, I. M., Tanke, H. J. & Dirks, R. W. Mobile foci of Sp100 do not contain PML: PML bodies are immobile but PML and Sp100 proteins are not. *J Struct. Biol.* **140,** 180–188 (2002).
27. Bloch, D. B. *et al.* Structural and functional heterogeneity of nuclear bodies. *Mol. Cell Biol.* **19,** 4423–4430 (1999).
28. Chang, K. S., Fan, Y. H., Andreeff, M., Liu, J. & Mu, Z. M. The *PML* gene encodes a phosphoprotein associated with the nuclear matrix. *Blood* **85,** 3646–3653 (1995).
29. Bulger, M. & Groudine, M. Looping versus linking: toward a model for long-distance gene activation. *Genes Dev.* **13,** 2465–2477 (1999).
30. Carter, D., Chakalova, L., Osborne, C. S., Dai, Y. F. & Fraser, P. Long-range chromatin regulatory interactions *in vivo*. *Nature Genet.* **32,** 623–626 (2002).
31. Spilianakis, C. G. & Flavell, R. A. Long-range intrachromosomal interactions in the T helper type 2 cytokine locus. *Nature Immunol.* **5,** 1017–1027 (2004).
32. Murrell, A., Heeson, S. & Reik, W. Interaction between differentially methylated regions partitions the imprinted genes *Igf2* and *H19* into parent-specific chromatin loops. *Nature Genet.* **36,** 889–893 (2004).
33. Volpi, E. V. *et al.* Large-scale chromatin organization of the major histocompatibility complex and other regions of human chromosome 6 and its response to interferon in interphase nuclei. *J. Cell Sci.* **113,** 1565–1576 (2000).
34. Hawkins, S. M., Kohwi-Shigematsu, T. & Skalnik, D. G. The matrix attachment region-binding protein SATB1 interacts with multiple elements within the gp91phox promoter and is down-regulated during myeloid differentiation. *J. Biol. Chem.* **276,** 44472–44480 (2001).
35. Kumar P. P. *et al.* Phosphorylation of SATB1, a global gene regulator, acts as a molecular switch regulating its transcriptional activity *in vivo*. *Mol Cell.* **22,** 231–243 (2006).
36. Bruno, S. *et al.* The *PML* gene is not involved in the regulation of MHC class I expression in human cell lines. *Blood* **101,** 3514–3519 (2003).
37. Larghero, J. *et al.* Alteration of the PML proto-oncogene in leukemic cells does not abrogate expression of MHC class I antigens. *Leukemia* **13,** 1295–1296 (1999).
38. Kumanovics, A., Takada, T. & Lindahl, K. F. Genomic organization of the mammalian MHC. *Annu. Rev. Immunol.* **21,** 629–657 (2003).
39. de Laat, W. & Grosveld, F. Spatial organization of gene expression: the active chromatin hub. *Chromosome Res.***11,** 447–459 (2003).
40. Kohwi-Shigematsu, T., de Belle, I., Dickinson, L. A., Galande, S., & Kohwi, Y. Identification of base-unpairing region (BUR)-binding proteins and characterization of their *in vivo* binding sequences. *Methods Cell Biol.* **53,** 323–354 (1998).
41. Seo, J., Lozano, M. M. & Dudley, J. P. Nuclear matrix binding regulates SATB1-mediated transcriptional repression. *J. Biol. Chem.* **280,** 24600–24609 (2005).
42. Dickinson, L. A., Joh, T., Kohwi, Y. & Kohwi-Shigematsu, T. A tissue-specific MAR/SAR binding protein with unusual binding site recognition. *Cell* **70,** 631–645 (1992).
43. Weis, K. *et al.* Retinoic acid regulates aberrant nuclear localization of PML-RAR α in acute promyelocytic leukemia cells. *Cell* **76,** 345–356 (1994).
44. Grande, M. A. *et al.* PML-containing nuclear bodies: their spatial distribution in relation to other nuclear components. *J. Cell Biochem.* **63,** 280–291 (1996).
45. Rampalli, S. *et al.* Stimulation of Tat-independent transcriptional processivity from the HIV-1 LTR promoter by matrix attachment regions. *Nucleic Acids Res.* **31,** 3248–3256 (2003).

Protein View

Match to: gi|4506791 Score: 37special AT-rich sequence binding protein 1 [Homo sapiens]
Found in search of KS_031103_PML_7_081103.pkl

Nominal mass (Mr): 85903; Calculated pI value: 6.10NCBI BLAST search of gi|4506791 against nrUnformatted sequence string for pasting into other applications

Taxonomy: Homo sapiensLinks to retrieve other entries containing this sequence from NCBIEntrez: gi|12804639 from Homo sapiensgi|417747 from Homo sapiensgi|337811 from Homo sapiens

Variable modifications: Carbamidomethyl (C),Oxidation (M)Cleavage by Trypsin: cuts C-term side of KR unless next residue is PSequence Coverage: 2%

Matched peptides shown in Bold Red

1 MDHLNEATQG KEHSEMSNNV SDPKGPPAKI ARLEQNGSPL GRGRLGSTGA
51 KMQGVPLKHS GHLMKTNLRK GTMLPVFCVV EHYENAIEYD CKEEHAEFVL101 VRKDMLFNQL IEMALLSLGY
SHSSAAQAKG LIQVGKWNPV PLSYVTDAPD151 ATVADMLQDV YHVVTLKIQL HSCPKLEDLP PEQWSHTTVR
NALKDLLKDM201 NQSSLAKECP LSQSMISSIV NSTYYANVSA AKCQEFGRWY KHFKKTKDMM251 VEMDSLSELS
QQGANHVNFG QQPVPGNTAE QPPSPAQLSH GSQPSVRTPL301 PNLHPGLVST PISPQLVNQQ LVMAQLLNQQ YAVNRLLAQQ
SLNQQYLNHP351 PPVSRSMNKP LEQQVSTNTE VSSEIYQWVR DELKRAGISQ AVFARVAFNR 401 TQGLLSEILR KEEDPKTASQ
SLLVNLRAMQ NFLQLPEAER DRIYQDERER451 SLNAASAMGP APLISTPPSR PPQVKTATIA TERNGKPENN TMNINASIYD501
EIQQEMKRAK VSQALFAKVA ATKSQGWLCE LLRWKEDPSP ENRTLWENLS551 MIRRFLSLPQ PERDAIYEQE SNAVHHHGDR
PPHIIHVPAE QIQQQQQQQQ601 QQQQQQQAPP PPQPQQQPQT GPRLPPRQPT VASPAESDEE NRQKTRPRTK651 ISVEALGILQ
SFIQDVGLYP DEEAIQTLSA QLDLPKYTII KFFQNQRYYL701 KHHGKLKDNS GLEVDVAEYK EEELLKDLEE SVQDKNTNTL
FSVKLEEELS751 VEGNTDINTD LKD

Peptides

Start-End Observed Mr(expt) Mr(calc) Delta Miss Sequence

386 - 395 510.2582 1018.5018 1018.5559 -0.0541 0 R.AGISQAVFAR.V
(Ions score 27)

511 - 518 432.2294 862.4442 862.4912 -0.0470 0 K.VSQALFAK.V
(Ions score 10)

b

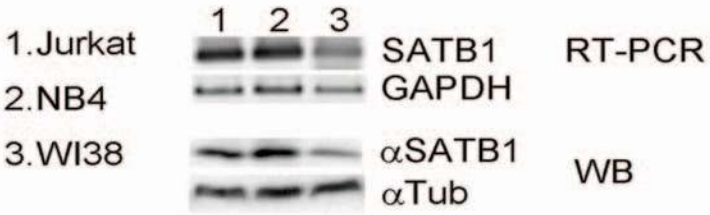

Figure S1 (a). Mass-spectrometric identification of SATB1 as a PML interacting protein. Anti-PML affinity column chromatography was performed to isolate proteins physically interacting with PML. Proteins in the eluate were resolved on SDS-PAGE, silver-stained and individual bands were excised and identified by peptide mass fingerprinting. Sequences of two tryptic peptides matched perfectly with that of human SATB1 as revealed from the Mascot search results depicted here. **(b).** Expression of SATB1 is not restricted to T cells. RT-PCR analysis of RNA isolated from Jurkat T cells, NB4 cells and WI38 fibroblast cells was performed to monitor expression of SATB1 or GAPDH as control (Top two panels). Immunoblot analysis of protein lysates from above cell lines using anti-SATB1 or anti-tubulin (loading control) (Bottom panels).

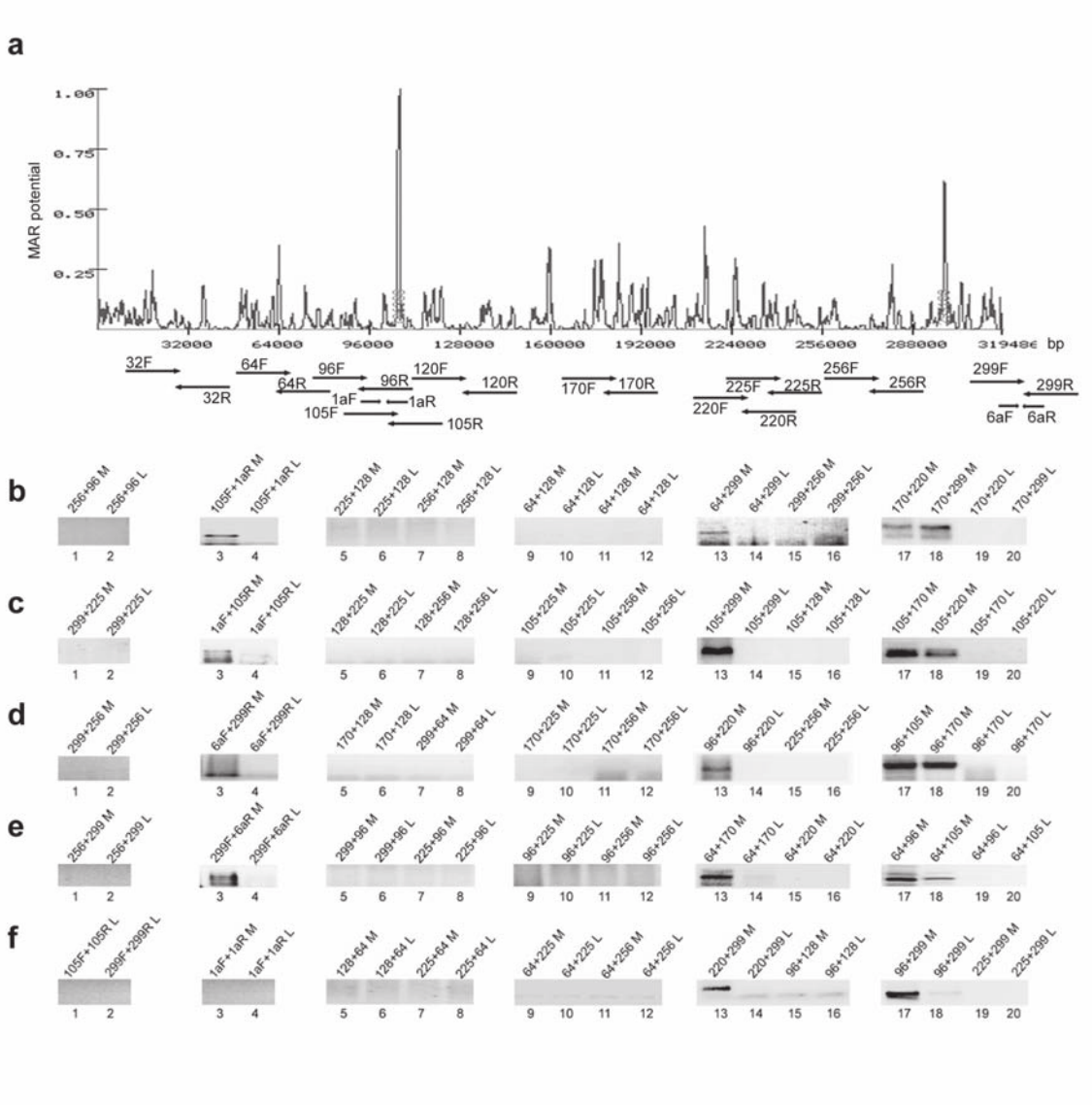

Figure S2 Chromatin loop configuration of the MHC I locus using matrix-loop assay. **(a)** Prediction of MARs. Putative MARs within the selected 300 kb region of human MHC I locus were identified utilizing the online tool 'MAR-Wiz' (Singh et al., 1997). The graph denotes MAR potential across this region in an arbitrary scale of 0 to1. Regions above a MAR potential of 0.5 were considered as candidates having strong nuclear matrix binding potential. Positions and designations of the primers used for analysis of matrix associated regions of MHC class I locus are as indicated. Primers are in the forward (F) or reverse (R) orientation. Smaller size arrows depict primer sets 1a and 6a that are internal to the region amplified by primer sets 105 and 299 respectively and were designed to specifically amplify the regions harboring the strong MARs at these positions. With the exception of 105F and 105R, all other primers essentially overlap within pairs. **(b-f)** MAR-ligation assay. Briefly, matrix (M) and loops (L) DNA was prepared as described in Methods. Matrix associated DNA fragments were purified followed by overnight ligation and used as a template for PCR with different combination of primers as follows: 105F-1aR primer (panel B lane 3), 1aF-105R (panel C lane 3) and 6aF-299R (panel D lane 3), 299F-6aR (panel E lane 3) primer sets only in matrix-bound, but not loop DNA templates. Using these regions as reference MARs we then looked at other putative regions within the MHC locus that are tethered to the matrix testing different primer sets in various combinations. The primer sets 64F-299R (panel B lane 13), 170F-220R (panel B lane 17), 170F-299R (panel B lane 18), 105F-299R (panel C lane 13), 105F-170R (panel C lane 17), 105F-220R (panel C lane 18), 96F-220R (panel D lane 13), 96F-105R (panel D lane 17), 96F-170R (panel D lane 18), 64F-170R (panel E lane 13), 64F-96R (panel E lane 17), 64F-105R (panel E lane 18), 220F-299R (panel F lane13), and 96F-299R (panel F lane 17) showed specific amplification only with the matrix-associated DNA demonstrating their *in vivo* association with the nuclear matrix. By contrast, DNA from chromatin loops, which are not adjacent to nuclear matrix, failed to render a specific PCR product confirming the specificity and accuracy of the experimental approach (panel B lanes 14, 19, 20; panel C lanes 14, 19, 20; panel D lanes 14, 19, 20; panel E lanes 14, 19, 20; panel F lanes 14 and 18).

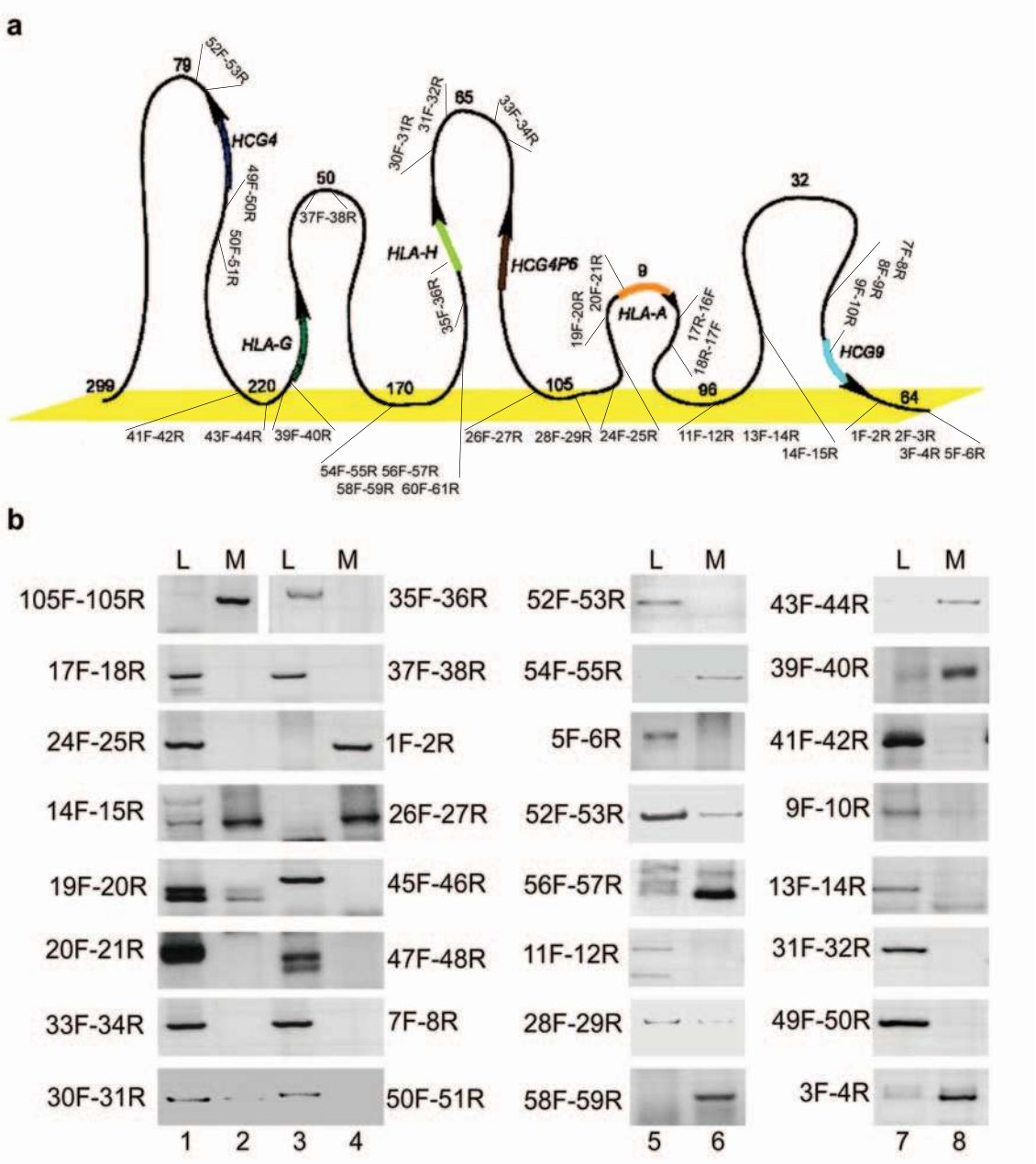

Figure S3 Preferential association of the MARs within the MHC locus with the nuclear matrix. **(a)** Schematic depiction of locations of various primers located in a 0.3 Mb region of the MHC class I locus within the human chromosome 6p21.3 locus flanked by the HLA-F and HCG-9 genes, respectively. **(b)** Matrix-loop partitioning assay. Matrix-bound (M) and loop-associated DNAs (L) were prepared as described in Methods. Purified DNAs were used as templates for PCR amplifications using primer pairs as indicated. Under these conditions, presence or absence of PCR amplification product can be directly correlated with the presence or absence of the corresponding genomic region in the respective compartment.

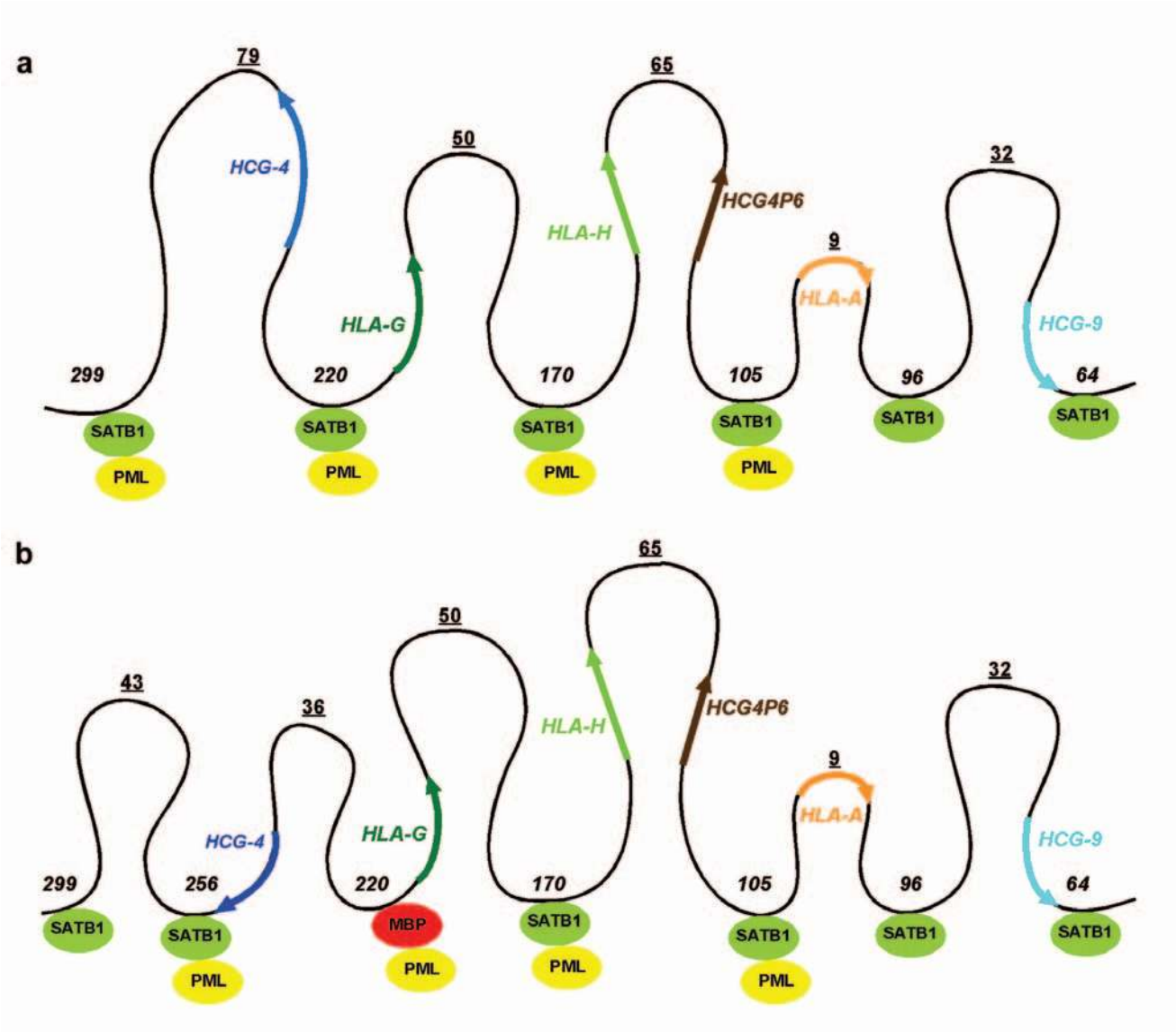

Figure S4 Schematic representation of the chromatin loop structure of the MHC class I locus in control cells **(a)** and IFNγ treated cells **(b)** as deduced from the ChIP-loop assay. Combined ChIP with the chromatin loop assay was performed as described in Methods. Base positions of MARs at the bases of each loop are indicated in kb. The numbers above each loop correspond to the loop size in kb. The attachments of proteins to the MARs at the bases of the loops as deduced by the ChIP-loop assay represented in Figure 5 are indicated by color coded balls. Green balls depict SATB1 and yellow balls PML. Unknown MAR-binding protein (MBP) tethering the region around 220 kb is represented in red. The shapes and sizes of the loops are only suggestive and over simplified for sake of visualization.

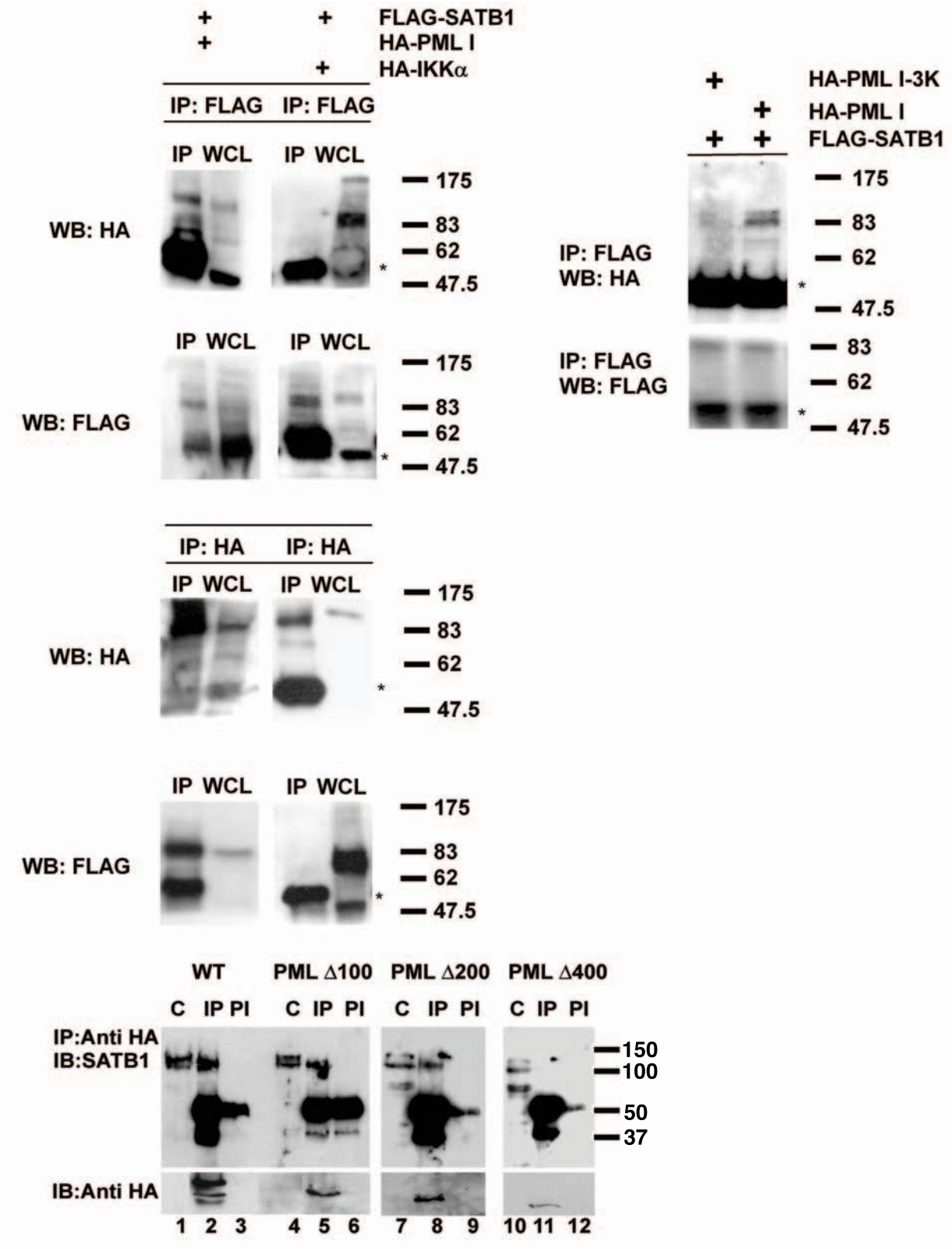

Figure S5 Full scans of the western blots presented in various panels of Fig. 1. Molecular weight standards in kDa are as indicated on side of each panel.